BioMetals (2006) 19:675–683
DOI 10.1007/s10534-006-9004-4

Oxidative renal tubular injuries induced by aminocarboxylate-type iron (III) coordination compounds as candidate renal carcinogens

Ryuichiro Mizuno[1,*], Teruyuki Kawabata[2], Yuichi Sutoh[3], Yuzo Nishida[3] & Shigeru Okada[1]

[1]*Department of Pathological Research, Okayama University Graduate School of Medicine and Dentistry, 2-5-1 Shikata-cho, Okayama, 700-8558, Japan;* [2]*Department of Applied Physics, Faculty of Science, Okayama University of Science, Okayama, Japan;* [3]*Chemical Institute for Neurodegeneration (CIN), Faculty of Science, Yamagata University, Yamagata, Japan; *Author for correspondence (Tel.: +81-86-235-7145; Fax: +81-86-235-7148; E-mail: mzn@bronze.ocn.ne.jp)*

Received 7 September 2005; accepted 10 March 2006

Key words: Iron, NTA, EDTA, IDA, μ-oxo dimer

Abstract

Oxidative renal tubular injuries and carcinogenesis induced by Fe^{III}-nitrilotriacetate (NTA) and Fe^{III}–ethylenediamine-*N,N′*-diacetate (EDDA) have been reported in rodent kidneys, but the identity of iron coordination structure essential for renal carcinogenesis, remains to be clarified. We compared renal tubular injuries caused by various low molecular weight aminocarboxylate type chelators with injuries due to NTA and EDDA. We found that Fe^{III}-iminodiacetate (IDA), a novel iron-chelator, induced acute tubular injuries and lipid peroxidation to the same extent. We also prepared Fe^{III}-IDA solutions at different pHs, and studied resultant oxidative injuries and physicochemical properties. The use of Fe^{III}-IDA at pH 5.2, 6.2, and 7.2 resulted in renal tubular necrosis and apoptotic cell death, but neither tubular necrosis nor apoptosis was observed at pH 8.2. Spectrophotometric data suggested that Fe^{III}-IDA had the same dimer structure from pH 6.2 to 7.2 as Fe^{III}-NTA; but at a higher pH, iron polymerized and formed clusters. Fe^{III}-IDA was crystallized, and this was confirmed by X-ray analysis and magnetic susceptibility measurements. These data indicated that Fe^{III}-IDA possessed a linear μ-oxo bridged dinuclear iron (III) around neutral pH.

Abbreviations: TUNEL – TdT-mediated dUTP nick end labeling; TBARS – thiobarbituric acid reactive substance; ESR – electron spin resonance

Introduction

Ferric nitrilotriacetate (Fe^{III}-NTA) is a well-known renal carcinogen, and Fe^{III}-NTA-injected animals have been used as a model of free-radical carcinogenesis (Iqbal *et al.* 2003; Mizote *et al.* 2002). Free radical injuries by repeated injections of Fe^{III}-NTA were clearly demonstrated, and resulted in renal carcinoma (Okada 1996, 2003). When Fe^{III}-NTA is intraperitoneally injected into animals, lipid peroxidation and oxidative modification of proteins and DNA occur in renal proximal tubules, and tubular epithelial cells are damaged (Toyokuni *et al.* 1993; Ma *et al.* 1997). Thiobarbituric acid reactive substance (TBARS) has also been shown to increase in kidneys, and cold Schiff's staining showed lipid peroxidation in renal proximal tubules (Okada *et al.* 1991) in Fe^{III}-NTA-treated animals. Increases in 4-hydroxy-2-nonenal (4-HNE)-modified proteins and 8-hydroxy-deoxyguanosine (8-OH-dG) were previously demonstrated using biochemical and

immunohistochemical methods (Toyokuni *et al.* 1994, 1996). In Fe^{III}-NTA-injected mice, amount of reduced glutathione decreased, and the oxidized form increased when metabolic rate of glutathione was accelerated (Okada *et al.* 1993). α-Tocopherol was shown to prevent the above Fe^{III}-NTA-induced renal injuries and carcinogenesis (Zhang *et al.* 1997).

Repeated injections of with Fe^{III}-NTA result in appearance of atypical epithelial cells in renal tubules, and finally in induction of renal carcinoma (Toyokuni 1996; Ma *et al.* 1998). Kawabata *et al.* (1997) reported that some damaged tubular cells disappeared from the tubules due to apoptosis in Fe^{III}-NTA injected mice. In addition, Hiroyasu *et al.* (2002) reported specific allelic loss of the p16 (INK4A) tumor suppressor gene in rats after a few weeks of repeated Fe^{III}-NTA injections. A few DNA-damaged cells that did not undergo apoptosis might have changed into renal carcinoma cells.

From all these previous studies, there is no doubt that Fe^{III}-NTA induces renal carcinoma through a free radical mechanism, and detailed molecular mechanisms of Fe^{III}-NTA-induced carcinogenesis are currently being clarified. However, chemical properties necessary for renal tubular injury and carcinogenesis remain unknown. We previously reported that Fe^{III}-EDDA showed the same effects as Fe^{III}-NTA in renal tubules, ultimately inducing renal carcinoma (Liu *et al.* 1994); other iron chelators such as Fe^{III}-citrate and -ADP, did not induce renal tubular injuries (Liu *et al.* 1991). Fe^{III}-NTA and –EDDA show spectrophotometric properties of a dimer iron structure (Nishida *et al.* 1995), and Fe^{III}-NTA was crystallized as a dimer iron with a μ-oxo and μ-carbonato bridge (Nshida *et al.* 1991). Therefore, we hypothesize that iron coordination compounds with a dimer structure are effective for renal carcinogenesis.

To prove our hypothesis of iron-induced carcinogenesis, we comprehensively screened various low molecular weight aminocarboxylate type iron chelators similar to NTA and EDDA, and investigated their effects on renal tubular injuries. We confirmed renal tubular injuries using hematoxylin-eosin staining and immunohistochemistry. Experimental results were compared with TBARS values as markers of lipid peroxidation, and apoptosis detection patterns obtained using *in situ* TUNEL staining. We identified Fe^{III}-IDA, a novel iron chelator, that induced oxidative renal tubular injuries. Treatment with Fe^{III}-IDA resulted in renal tubular damage at pH 5.2, 6.2, and 7.2, but neither tubular necrosis nor apoptosis was observed at pH 8.2. The coordination structure of Fe^{III}-IDA was investigated by UV–Vis and ESR spectra of the chelator in solution, and in serum at different pHs. Elemental analysis, single crystal X-ray study, and magnetic susceptibility analysis of crystallized Fe^{III}-IDA were performed for chemical structure determination.

Materials and methods

Reagents

Nitrilotriacetic acid (disodium salt; NTA) was purchased from Sigma Chemical Co. (St Louis, MO, USA). All other chelators were of the highest quality, and were available from Wako Pure Chemicals Co., Ltd (Osaka, Japan). Iron chelators were prepared just prior to use, according to the Fe^{III}-NTA preparation method, as previously described (Awai *et al.* 1979). Iron concentration was 1 mg/ml, molar ratio of iron to chelator was 1:4, and pH was adjusted with sodium bicarbonate (Ishizu, Japan).

In vivo experiments

Six-week-old male Wistar rats weighing 130–150 g were obtained from the Shizuoka Laboratory Animal center (Shizuoka, Japan), and were fed with standard laboratory food (Oriental Yeast Industry, Osaka, Japan) and water *ad libitum*. Animals were randomly divided into control groups and iron-injected groups (5–7 animals in each group). Iron chelators or an equivalent dose of the corresponding chelator without iron (controls) were intraperitoneally injected into rats at a dose of 7.5 mg Fe/kg body weight. Rats were euthanatized 6 h after injection, and kidneys were promptly removed for histological and biochemical analyses. Serum was centrifuged after coagulation for 10 min at 3000 rpm. Serum iron concentration and iron binding capacity of tranferrin were measured using an internationally standardized method (Goodwin *et al.* 1966).

Morphological study and quantification

Rat kidneys were fixed in 20% buffered formalin overnight, and were embedded in paraffin following tissue processing. Then, thin sections were prepared using routine methods, and were stained with hematoxylin and eosin. Apoptotic cells were detected *in situ* by TUNEL staining with a TREVIGEN TUNEL detection kit (MD, USA) according to the manufacturer's protocols. Numbers of TUNEL-positive cells were assessed by two pathologists in five random×200-magnification fields. The number of positive cells in each 100 cells was quantified in three different blocks.

Deoxyribose degradation assay

Deoxyribose degradation was assayed using the method of Halliwell *et al*. (1987). Deoxyribose (0.2 ml, 5 mM), 0.2 ml 100 mM H_2O_2, and 0.1 mM catalase as an inhibitor for decomposition of H_2O_2 were mixed together. Then, 100 μM ascorbic acid was added, and the reaction was started by addition of 0.1 mM iron chelator. After incubation at 37 °C for 60 min, 0.2 ml 1% TBA in 50 mM NaOH were added, followed by 0.2 ml 2.8% trichloroacetate, and the mixture was heated at 100 °C for 10 min. The resulting pink chromogen was extracted with 4 ml *n*-butanol, and its concentration was measured spectrometrically at 532 nm. Iron chelators and ascorbic acid were prepared immediately prior to each experiment. pH was adjusted to 7.2 with sodium bicarbonate.

Measurement of lipid peroxidation

We measured TBARS content in kidneys to assess lipid peroxidation, as previously described (Ohkawa *et al*. 1979). Values were expressed in nM malondialdehyde/100 mg tissue, and were calibrated with the external standard 1,1,3,3-tetramethoxypropane (Sigma Chemical Co., Ltd. St Louis, MO, USA).

Spectrophotometric analysis

UV/Vis absorption spectra were measured at room temperature with a Hitachi UV/Vis absorption spectrophotometer (Ibaragi, Japan). ESR spectra were recorded at 77 K with a JES-PX2300 ESR spectrometer (JOEL Co. Ltd, Tokyo, Japan). All other conditions are stated in appropriate figure legends.

Structural determination

By adding methanol to the Fe^{III}-IDA solution ([IDA]/[Fe^{3+}] = 4, pH = 7.0), brown solids were obtained. These were then recrystallized from a water/methanol (1/1) solution to give brown crystals. Elemental analyses of carbon, hydrogen, and nitrogen were conducted with a Yanako MT-5 CHN recorder (Kyoto, Japan). Single crystal X-ray analyses were performed with a Rigaku X-ray analysis system RASA-7R (Tokyo, Japan), and the crystal structure was shown by Oak Ridge Thermal Ellipsoid Plot (ORTEP) drawing. Magnetic susceptibilities were measured using the Faraday method over a temperature range of 87–293 K (Saga University, Japan). Bohr magnetic moments were calculated to determine the ligand structure.

Results

Acute tubular injuries caused by various chelators similar to NTA and EDDA were examined in the present study (Figure 1). All chelators contained amine and carboxyl groups able to bind to ferric ions at physiological pH. We prepared all iron chelators just prior to use, according to the methods of Awai *et al*., and injected them into the rats' peritoneum. Renal tubular necrosis was analyzed by routine H/E staining, and was compared with those induced by Fe^{III}-NTA and -EDDA. Cytotoxic chelator-induced renal tubular necrosis developed 6 h after intraperitoneal injection (Figure 2). Fe^{III}-IDA at pH 5.2, 6.2, and 7.2 caused renal proximal tubule necrosis to similar extents as Fe^{III}-NTA and –EDDA; however, at pH 8.2, Fe^{III}-IDA did not induce tubular necrosis. Other chelators did not induce tubular necrosis.

To qualitatively assess renal injuries, we measured level of TBARS in the kidneys. Figure 3 shows TBARS level in kidneys 6 h after iron injection. Fe^{III}-IDA at pH 6.2 and 7.2 resulted in the same TBARS amount as with Fe^{III}-NTA, and this amount decreased with increasing pH as stated above. Fe^{III}-IDA at pH 8.2 showed the same amount of TBARS as the control. Apoptotic cell death in renal tubules was assessed after Fe^{III}-IDA

NTA; nitrilotriacetate

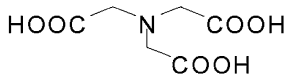

EDTA-OH; *N*-(2-hydroxyethyl) ethylenediamine -*N,N'*-triacetate

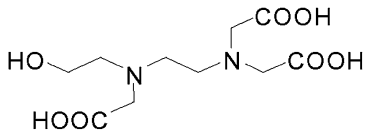

EDDA; ethylenediamine-*N,N'*-diacetate

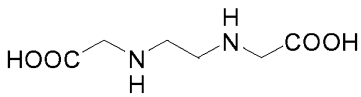

HIDA; *N*-(2-hydroxyethyl)iminodiacetate

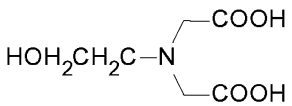

IDA; iminodiacetate

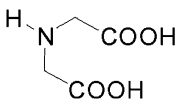

EDDP; etylenediamine-*N,N'*-dipropionate

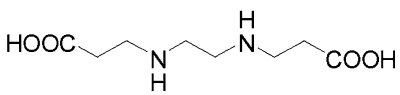

EDTA; ethylenediamine-*N,N'*-tetraacetate

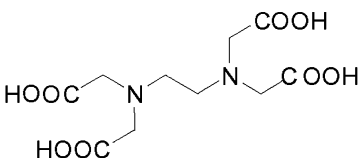

HBED; *N,N'*-bis(2hydroxybenzyl)ethylenediamine -*N,N'*-diacetate

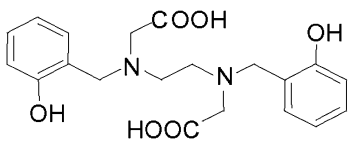

Figure 1. Chemical structure of the aminocarboxylate type chelator used in this study.

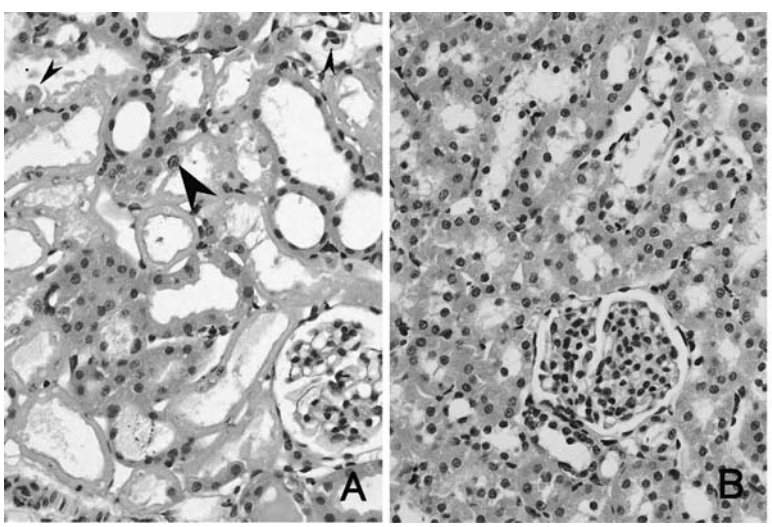

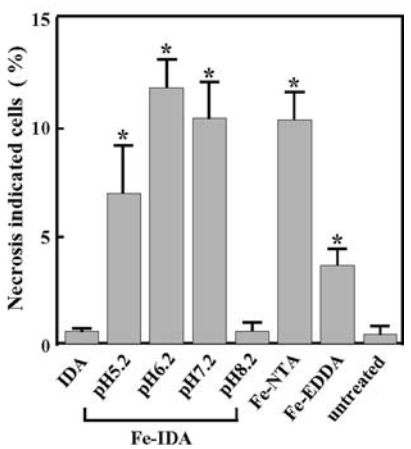

Figure 2. Proximal tubules necrosis in rat kidneys 6 h after injection of (A) Fe^{III}-IDA at pH 6.2, (B) Fe^{III}-IDA at pH 8.2. Hematoxylin and eosin staining (magnification, ×100). Proximal tubular cells were specifically destroyed by Fe^{III}-IDA at pH 5.2, 6.2, and 7.2. Effects of Fe^{III}-IDA at pH 8.2 were not observed. Patchy degeneration of the proximal tubular epithelium with pyknotic nuclei (*small arrowheads*). Regenerative cells are large and irregularly shaped with prominent nucleoli (*large arrowheads*). These cells were quantitated for necrotic cells. Data are presented as means ±SD (5–7 animals). *Significantly different ($P < 0.05$).

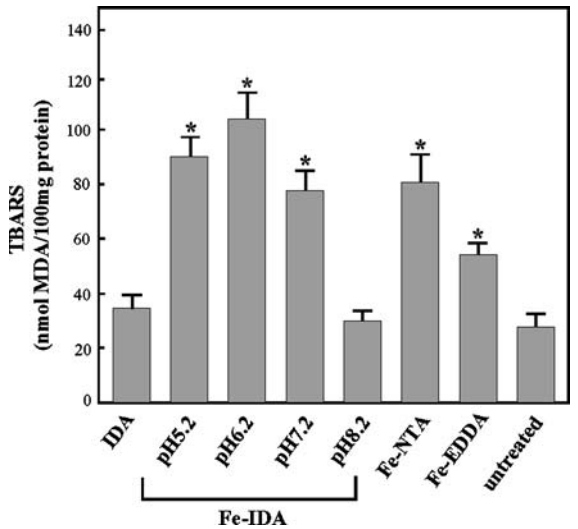

Figure 3. Effects of different pHs on TBA reactivity in Fe^{III}-IDA-injected rat kidneys. The assay was performed as described in Materials and Methods. Data are presented as means ±SD (5–7 animals). *Significantly different ($P < 0.05$).

injection. Apoptotic cells were detected as TUNEL-positive cell nuclei in rat renal tubules injected with Fe^{III}-IDA at pH 5.2, 6.2, and 7.2; but in renal tubules injected with Fe^{III}-IDA at pH 8.2, there were no TUNEL-positive cells (Figure 4). Fe^{III}-IDA at pH 5.2, 6.2, and 7.2 induced DNA damage in renal tubules, and tubular cells underwent apoptosis. However, at pH 8.2, Fe^{III}-IDA did not induce DNA damage. Fe^{III}-EDTA with ascorbic acid was significantly detected via deoxyribose degradation. Fe^{III}-NTA, -EDDA, and -IDA were significantly degraded without ascorbic acid, and were inhibited by catalase (Figure 5).

We studied the molecular environments of Fe^{III}-IDA solutions at varying pHs using UV–Vis absorbance and ESR spectroscopy. With regards to UV–Vis absorbance, characteristic absorption similar to that of the Fe^{III}-NTA solution appeared at around 440 nm, and revealed a shoulder at 480 nm (Figure 6A). With ESR, a peak at $g = 4.60$ was predominantly recorded in the Fe^{III}-IDA solution at pH 5.2; this was derived from mononuclear iron chelators. As the pH of the Fe^{III}-IDA solution increased, the signal decreased, and the ESR signal was generally silent from pH 6.2 to 7.2. At a higher pH, a smaller signal remained at a little higher magnetic field (Figure 6B). Decrease in the mononuclear signal at around neutral pH was very similar to that seen with pH-dependent changes of Fe^{III}-NTA.

Serum iron concentration was almost the same at each pH after Fe^{III}-IDA injection (Figure 7). Fe^{III}-NTA, -EDDA, and -EDTA also showed the same iron concentration as Fe^{III}-IDA. Iron level far exceeded total iron binding capacity (TIBC) of transferrin (data not shown). ESR spectra in serum 1 h after Fe^{III}-IDA injection is shown in Figure 8. The $g = 4.3$ signal derived from the mononuclear complex was observed with injection of a pH 5.2- solution. Following Fe^{III}-IDA injection around neutral pH, only the transferrin signal was observed. An unknown signal around $g = 2.0$ appeared after injection of a higher pH solution,

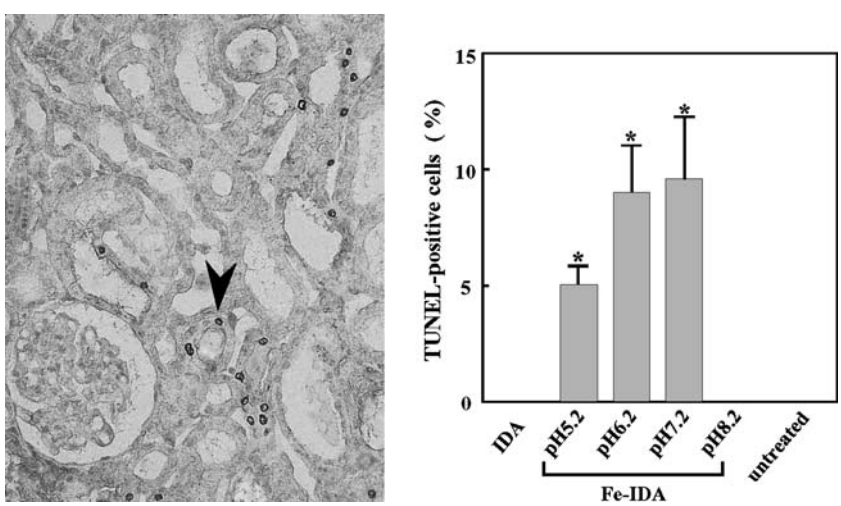

Figure 4. *In situ* end-labeling (TUNEL staining) in rat renal tissues after Fe^{III}-IDA injection at pH 6.2 (magnification, ×100). The arrowheads indicate TUNEL-positive cells. Apoptotic cells are observed in the proximal tubules of Fe^{III}-IDA (pH 5.2, pH 6.2, and pH 7.2)-injected rat kidneys. Data are presented as means ±SD (5–7 animals). *Significantly different ($P < 0.05$).

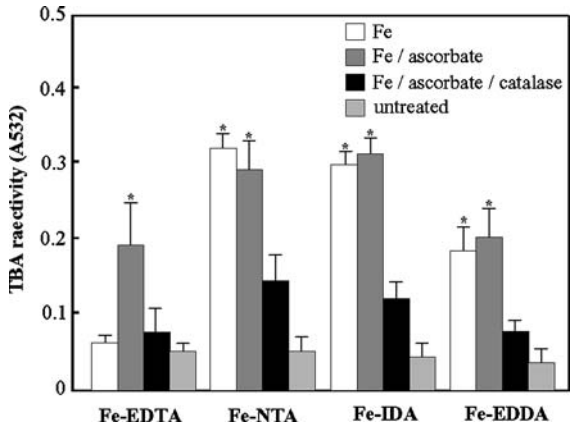

Figure 5. Comparisons of effects between different Fe^{III}-chelators on deoxyribose degradation. The assay was performed as described in Materials and Methods. Fe, Fe^{III}-chelator is □; Fe/ascorbate, Fe^{III}-chelator and ascorbate is ■; Fe/ascorbate/catalase, Fe^{III}-chelate and ascorbate and catalase is ■; untreated control is ■. Results represent means ±SD ($n=6$). *Significantly different ($P<0.05$).

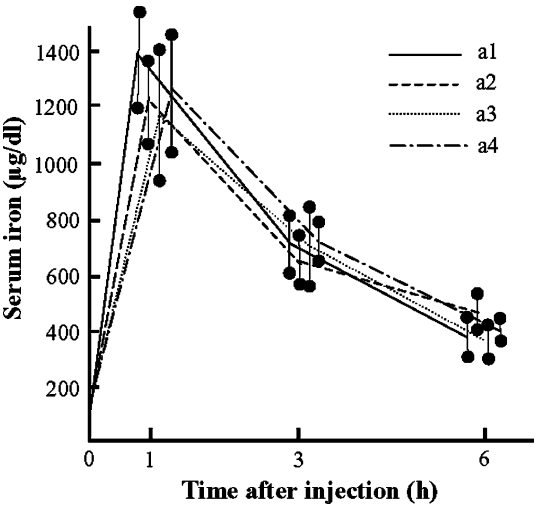

Figure 7. Serum iron concentration after a single intraperitoneal injection of Fe^{III}-IDA (7.5 mg Fe/kg body weight): (a1) pH 5.2, (a2) pH 6.2, (a3) pH 7.2, (a4) pH 8.2. Results represent means ±SD of each group (3–5 animals).

and the signal was not observed in Fe^{III}-IDA solutions.

Composition of elements in the crystallized form of Fe^{III}-IDA at pH 7.0 was also determined: C, 21.57%; H, 3.95%; and N, 6.28%, and was practically calculated for $Fe_2(O)(ida)_4Na_4(H_2O)_8$: C, 21.64%; H, 4.09% and N, 6.31%. Bohr magnetic moments of the compound were 2.15 and 1.07 BM at 293 and 86.7 K, respectively; and the magnetic property of this complex could be reasonably explained based on the theoretical expression for the binuclear iron (III) complex with $J=-84.8\ cm^{-1}$. These data suggested that this complex was derived from a binuclear iron (III) structure with an oxo-bridge (Tkahashi *et al.* 1985). The chemical structure of the crystallized Fe^{III}-IDA at pH 7.0 was obtained using single crystal X-ray analysis (Figure 9).

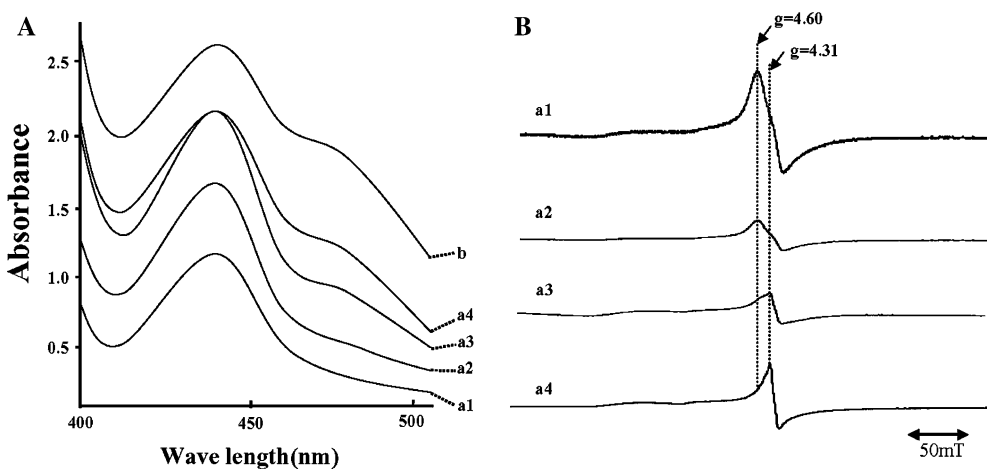

Figure 6. UV–Vis absorption and ESR spectra of iron chelator solutions. (A) UV–Vis absorption spectra of (a1) Fe^{III}-IDA at pH 5.2, (a2) Fe^{III}-IDA at pH 6.2, (a3) Fe^{III}-IDA at pH 7.2, (a4) Fe^{III}-IDA at pH 8.2, and (b) Fe^{III}-NTA were recorded at room temperature with a Hitachi UV/Vis absorption spectrophotometer (Ibaragi, Japan). (B) ESR spectra of these iron chelator solutions were recorded at 77 K with a JOEL JES-PX2300 ESR spectrometer (Tokyo, Japan) under the following conditions: frequency, 9.038 GHz; microwave power, 5.0 mW; modulation width, 0.06 mT; sweep time, 4.0 min; amplitude, 100.

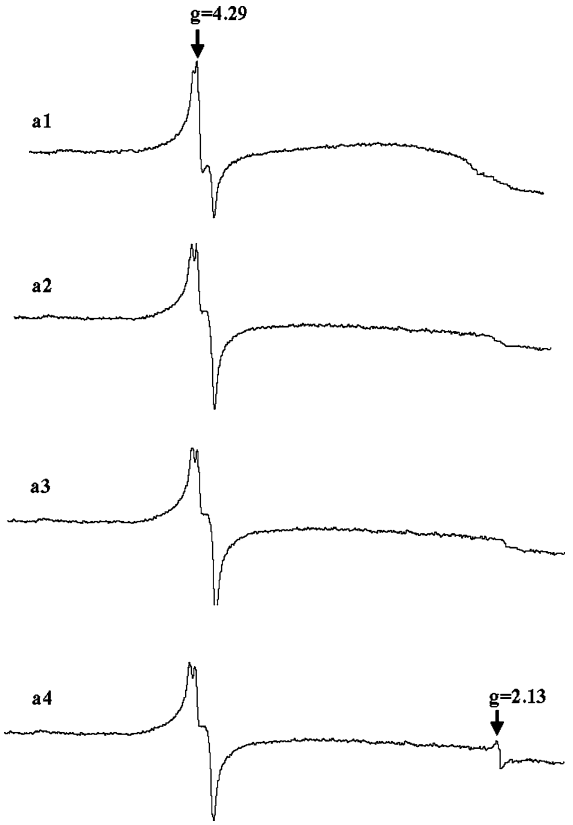

Figure 8. ESR spectra of serum 1 h after Fe^{III}-IDA injection: (a1) pH 5.2, (a2) pH 6.2, (a3) pH 7.2, (a4) pH 8.2. ESR spectra were recorded at 77 K with a JOEL JES-PX2300 ESR spectrometer (Tokyo, Japan) under the following conditions: frequency, 9.036 GHz; microwave power, 5.0 mW; modulation width, 0.6 mT; sweep time, 4.0 min; amplitude, 200.

Discussion

Determination of the coordination structure of iron chelators that promote carcinogenesis is the most important key in understanding chemical carcinogenesis, and its prevention. We previously reported two kinds of chelators that induced renal carcinoma: Fe^{III}-NTA and -EDDA. Because of physicochemical data, we hypothesized that the μ-oxo dimer structure was essential for iron-induced free radical injuries, and ensuing carcinogenesis. Chemically, this structure has been reported to be a pivotal structure required for dioxide activation (Nishida 1989), because hydrogen peroxide attached to a dimer iron acquires strong electrophilicity, and makes an electrophilic attack on biomolecules (Nishida 1999).

We assessed several iron chelators similar to NTA and EDDA for their ability to induce renal

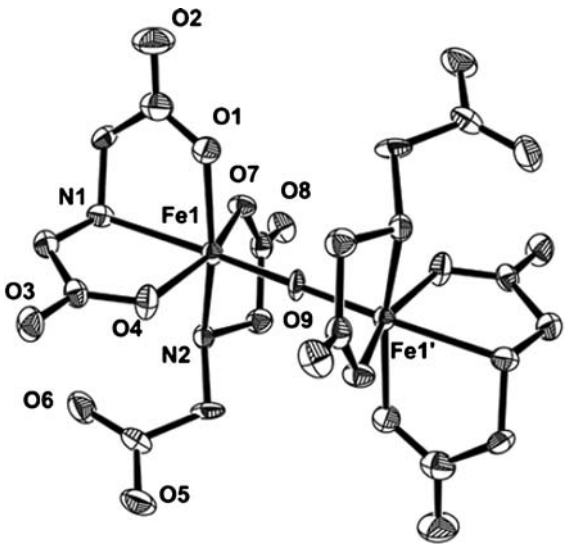

Figure 9. Chemical structure of the μ-oxo bridged dimer iron in crystallized Fe^{III}-IDA at pH 7.0 by ORTEP drawing of $[Fe_2O(IDA)_4]^{4-}$ ion.

tubular injuries (Figure 1). In addition to Fe^{III}-NTA and -EDDA, Fe^{III}-IDA induced severe renal tubular injuries in rat kidneys. Crystallized Fe^{III}-IDA at pH 7.0 contained a μ-oxo bridged dimer iron according to X-ray magnetic susceptibility analyses. From solution UV–Vis absorption spectrum analysis, Fe^{III}-IDA had almost the same spectrum as Fe^{III}-NTA, and showed the same absorption at around 440 nm with a shoulder at 480 nm (Figure 6A), which was assigned to a charge-transfer transition from the μ-oxo ligands to a d orbital of Fe^{III} (Donald *et al*. 1990; Que *et al*. 1990). Around neutral pH, ESR signals were silent, indicating the presence of a dimer structure of Fe^{III}-IDA, and anti-ferromagnetism (Carl *et al*. 1995). In solution, Fe^{III}-IDA also existed in a μ-oxo dimer iron at neutral pH.

This might also be true in rat serum. Ferric iron is ligand exchange-labile in solution. Blood pH is tightly maintained at pH 7.4, and thus Fe^{III}-IDA can easily exchange with other ligands. In fact, ferric iron was rapidly transferred to serum transferrins, and residual excess iron was in the mononuclear form after injection of the pH 5.2 Fe^{III}-IDA solution. However, in sera after injection of higher pH solutions, we did not observe the mononuclear iron. Since iron concentration was the same, the ESR-silent iron was present in sera, indicating that Fe^{III}-IDA had a dimer structure or a more aggregated one. A new broad signal

around $g = 2.0$ appeared after injection of the pH 8.2 solution, which possibly derived from a cluster complex with $s = 1/2$ (Hearth *et al.* 1992). Therefore, in rat sera, Fe^{III}-IDA may also exist in a μ-oxo dimer iron at neutral pH.

Finally, we would like to discuss differences between free radical injuries induced by a μ-oxo dimer iron, and the so-called Fenton-type reaction (Engelmann *et al.* 2003). Fe^{III}-EDTA is reported to be a mononuclear iron complex inducing DNA cleavage and lipid peroxidation with hydrogen peroxide, under reducing conditions (Wei *et al.* 2001; Yuan *et al.* 1995). Hydroxyl radicals were generated from the mixture of Fe^{III}-EDTA, ascorbic acid, and H_2O_2 through the Fenton reaction. In deoxyribose degradation by Fe^{III}-EDTA, not only H_2O_2, but also ascorbic acid was necessary. However, Fe^{III}-NTA, -EDDA, and -IDA degraded deoxyribose without reducing agents, and degradation was inhibited by catalase. These data suggested that Fe^{III}-NTA, -EDDA, and -IDA showed proper catalytic characteristics of H_2O_2 different from mononuclear iron chelators such as Fe^{III}-EDTA.

It is possible that nearly all iron chelators with a small molecular weight are filtered from renal glomeruli, and are excreted into the tubules, that is, glomerular filtration rates of these iron chelators may be the same. Distribution of iron chelators in renal tubules might not differ for different iron chelators due to their similar iron concentration in sera, and different effects of iron chelators must be related to different catalytic effects depending on iron coordination structure. In this study, we suggest that a dinuclear iron (III) coordination compound with a μ-oxo bridge is important in renal tubular injury and carcinogenesis.

Acknowledegments

We are very grateful to Prof. S. Yamazaki (Department of Fundamental Science, Okayama University of Science) for his helpful discussion, and Prof. T. Tokii (Department of Physical and Inorganic Chemistry, Saga University) for measuring magnetic susceptibility.

References

Awai M, Narasaki M, Yamanoi Y, Seno S. 1979 Induction of diabetes in animals by parenteal administration of ferric nitrilotriacetate. *Am J Pathol* **95**, 663–674.

Carl AB, Glenn JR, Ronald LM, Edward IS. 1995 Spectroscopic and electronic structure studies of met-hemerythrin model complexes: A description of the ferric-oxo dimer bond. *Inorg Chem* **34**, 688–717.1.

Donald M, Kurtz Jr. 1990 Oxo- and hydroxo-bridged diiron complexes: a chemical perspective on abiological unit. *Chem. Rev.* **90**(4), 585–606.

Engelmann MD, Babior RT, Hiatt T, Cheng IF. 2003 Variabirity of the Fenton reaction characteristics of the EDTA, DTPA and citrate complexes of iron. *Biometals* **16**, 519–527.

Goodwin JF, Marphy B, Guillemette M. 1966 Direct measurement of serum iron and binding capacity. *Clin Chem* **12**, 47.

Halliwell B, Gtteridge JMC, Aruoma OI. 1987 The deoxyribose method: a simple 'test-tube' assay for determination of rate constants for reactions of hydroxyl radicals. *Anal Biochem* **165**, 215–219.

Hearth SL, Powell AK. 1992 The trapping of iron hydroxide units by the ligand (hida): Two new hydroxo(oxo)iron clusters containing 19 and 17 iron atoms. *Angew Chem* **31**, 191–193.

Hiroyasu M, Ozeki M, Kohda H, Eshizenya M, Tanaka T, Hiai H, Toyokuni S. 2002 Specific allelic loss of p16 (INK4A) tumor suppressor gene after weeks of iron-mediated oxidative damage during rat renal carcinogenesis. *Am J Pathol* **160**, 419–424.

Iqbal M, Sharma SD, Mizote A, Fujisawa M, Okada S. 2003 Differential role of hydrogen peroxide and organic hydroperoxides in augmenting ferric nitrilotriacetate (Fe-NTA)-mediated DNA damage: implications for carcinogenesis. *Teratog Carcinog Mutagen l* **1**, 13–21.

Kawabata T, Ma Y, Yamador I, Okada S. 1997 Iron-induced apoptosis in mouse renal proximal tubules after an injection of a renal carcinogen, iron-nitrilotriacetate. *Carcinogenesis* **18**, 1389–1389.

Liu M, Okada S. 1994 Induction of free radicals and tumors in the kidneys of Wistar rats by ferric ethylenediamine-N,N′-diacetate. *Carcinogenesis* **15**, 2817–2821.

Liu M, Okada S, Kawabata T. 1991 Radical-promoting "free" iron level in the serum of rats treated with ferric nitrilotriacetate: comparison with other iron chelate complexes. *Acta Med Okayama* **45**, 401–408.

Ma Y, Zhang D, Kawabata T, Kiriu T, Toyokuni S, Uchida K, Okada S. 1997 Copper and iron-induced oxidative damage in non-tumor bearing LEC rats. *Pathol Int* **47**, 203–208.

Ma Y, Kawabata T, Hamazaki S, Ogino T, Okada S. 1998 Sex differences in oxidative damage in ddY mouse kidney treated with a renal carcinogen, iron nitrilotriacetate. *Carcinogenesis* **19**, 1983–1988.

Mizote A, Hida A, Hosako M, Fujisawa M, Kamekawa M, Okada S. 2002 Effects of phlebotomy on the growth of ferric nitrilotriacetate-induced renal cell carcinoma. *Acta Med Okayama* **56**, 199–204.

Nishida Y, Ito S. 1995 Structures and reactivities of several iron (III) complexes in the presence of hydrogen peroxide: relevance to induction of tissue damage caused by iron (III) chelastes in rats. *Polyhedron* **14**, 2301–2308.

Nishida Y, Akamatu T. 1991 Preparation of iron (III) complex with nitrilotriacetic acid and origin of its unique reactivity. *Chem Lett* 1521–1524.

Nishida Y. 1989 DNA cleavage by binuclear iron(III)-peroxide adducts. *Inorg chem Acta* **163**, 9–10.

Nishida Y. 1999 Structure and function of free iron ion in biological system and their model compounds. *Recent Res Devel Pure Applied Chem* **3**, 103–122.

Ohkawa H, Ohnishi N, Yagi K. 1979 Assay for lipid peroxides in animal tissues by thiobarbituric acid reaction. *Anal Biochem* **95**, 351–358.

Okada S. 2003 Prevention of free-radical mediated tissue damage and carcinogenesis induced by low-molecular-weight iron. *Biometals* **16**, 99–101.

Okada S, Fukunaga Y, Hamazaki S, Yamada Y, Toyokuni S. 1991 Sex differences in the localization and severity of ferric nitrilotriacetate-induced lipid peroxidation in the mouse kidney. *Acta Pathol Jpn* **41**, 221–6.

Okada S, Minamiyama Y, Hamazaki S, Toyokuni S, Sotomatu A. 1993 Glutathione cycle dependency of ferric nitrilotriacetate-induced lipid peroxidation in mouse proximal renal tubules. *Arch Biochem Biophys* **301**, 138–42.

Okada S 1996 Iron-induced tissue damage and cancer: the role of reactive oxygen species-free radicals. *Pathol Int* **46**, 311–32.

Que L Jr, True AE. 1990 Dinuclear Iron- and Manganese-Oxo Sites in Biology. *Prog Inorg Chem* **38**, 97–200.

Takahashi K, Nishida Y, Maeda Y. 1985 Crystal structure and magnetism of binuclear iron (III) complexes with a linear oxo-bridge. *J Chem Soc Dalton Trans* 2375–2380.

Toyokuni S, Uchida K, Okamoto K. 1994 Formation of 4-hydroxy-2-nonenal-modified proteins in the renal proximal tubules of rats treated with a renal carcinogen, ferric nitrilotriacetate. *Proc Nat Acad Sci USA* **91**, 2616–2620.

Toyokuni S, Sagripanti JL 1996 Association between 8-hydroxy-2′-deoxyguanosine formation and DNA strand breaks mediated by copper and iron. *Free Radic Biol Med* **20**, 859–864.

Toyokuni S, Sagripanti JL. 1993 DNA single- and double-strand breaks produced by ferric nitrilotriacetate in relation to renal tubular carcinogenesis. *Carcinogenesis* **14**, 223–227.

Toyokuni S. 1996 Iron-induced carcinogenesis: The role of redox regulation. *Free Radic Biol Med* **20**, 553–566.

Wei RR, Richardson JP. 2001 Identification of an RNA-binding Site in the ATP binding domain of Escherichia coli Rho by H_2O_2/Fe-EDTA cleavage protection studies. *J Biol Chem* **276**(30), 28380–28387.

Yuan XM, Brunk UT, Olsson AG 1995 Effects of iron- and hemoglobin-loaded human monocyte-derived macrophages on oxidation and uptake of LDL. *Arterioscler Throm Vas Biol* **15**(9), 1345–1351.

Zhang D, Okada S, Yu Y, Zheng P, Ymaguchi R, Kasai H. 1997 Vitamin E inhibits apoptosis, DNA modification, and cancer incidence induced by iron-mediated peroxidation in Wistar rat kidney. *Cancer Res* **57**, 2410–2414.